Available online at www.sciencedirect.com

ScienceDirect

Journal of the European Ceramic Society 29 (2009) 2355–2361

www.elsevier.com/locate/jeurceramsoc

Facile synthesis of bimetallic carbonitrides, $V_{1-x}Ti_x(C,N)$, by microwave carbothermal reduction–ammonolysis/carburisation (MW-CRAC) methods

Colin P. West[a,b], Ian Harrison[b], Edmund J. Cussen[c], Duncan H. Gregory[d,*]

[a] School of Chemistry, University of Nottingham, University Park, Nottingham NG7 2RD, UK
[b] Department of Electronic and Electrical Engineering, University of Nottingham, University Park, Nottingham NG7 2RD, UK
[c] WestCHEM, Department of Pure and Applied Chemistry, University of Strathclyde, Glasgow G1 1XL, UK
[d] WestCHEM, Department of Chemistry, University of Glasgow, Glasgow G12 8QQ, UK

Received 29 August 2008; received in revised form 5 January 2009; accepted 13 January 2009
Available online 13 February 2009

Abstract

New quaternary carbide nitrides in the $V_{1-x}Ti_x(C,N)$ ($0 \le x \le 0.4$) system have been synthesised rapidly (0.5–1.5 h) by carbothermal reduction, carburisation and ammonolysis *via* microwave heating using a custom-modified, multimode cavity microwave reactor. The products were structurally characterised by powder X-ray diffraction (PXD), while scanning electron microscopy (SEM) and energy dispersive X-ray analysis (EDX) were used to examine morphology and composition. The resulting carbonitrides crystallise with the rock salt structure and the cubic lattice parameters vary linearly with increasing titanium concentration (x), hence following Vegard's law. Particle sizes typically range from 250 nm to 2 μm.

Keywords: Microwave processing; Powders-solid state reaction; Carbides; Nitrides; Transition metals

1. Introduction

Metal carbides and nitrides find utility in a wide range of applications. Many display high melting points, hardness, strength and tribological properties that make them attractive for use in cermets and as coatings.[1,2] Magnetic and electronic properties have also been investigated,[3] with relevance for use in high temperature electronic devices.[4] Early transition metal (TM) nitrides and carbides also form an exciting and developing class of catalysts that exhibit high activity, selectivity and stability, particularly for industrially important hydrotreating processes, where they have been found to display surface electronic behaviour similar to that of the precious metal catalysts traditionally used, such as platinum and palladium.[5]

Many binary carbides and nitrides with the sodium chloride structure show complete mutual solubility, forming a continuous series of solid solutions[6] and are stable over a wide range of sub-stoichiometries.[7] There is scope for enhancing the properties of these materials and other comparable TM carbides and nitrides by compositional variation over a potentially huge range of ternary and quaternary compositions. The variation in properties with composition for a limited number of bimetallic carbides and nitrides has been reported and, for example, $Ti_{0.6}Hf_{0.4}C$ is among the hardest of known materials (43.1 GPa).[7] Likewise, monometallic carbonitrides such as $Ti(C_xN_{1-x})$ can show superior properties compared with the corresponding binary carbides and nitrides.[8] There remain a huge variety of ternary and quaternary compositions that require further investigation, particularly with regard to enhancing mechanical, electronic and catalytic properties, for example.

The use of microwave synthesis in solid-state chemistry and materials science has received significant recent attention.[9,10] These methods offer some notable alternatives and some considerable advantages when compared to conventional heating and particularly: drastically reduced reaction times, selectivity in the energy transfer to reactants, reduced energy consumption, rapid heating without temperature gradients in reagents/mixtures[11] and increased densification of products.[12] Reducing temperature gradients may be especially advantageous in the synthesis of interstitial TM carbides and nitrides in overcoming diffusion

---

[*] Corresponding author.
E-mail address: D.Gregory@chem.gla.ac.uk (D.H. Gregory).

0955-2219/$ – see front matter © 2009 Elsevier Ltd. All rights reserved.
doi:10.1016/j.jeurceramsoc.2009.01.018

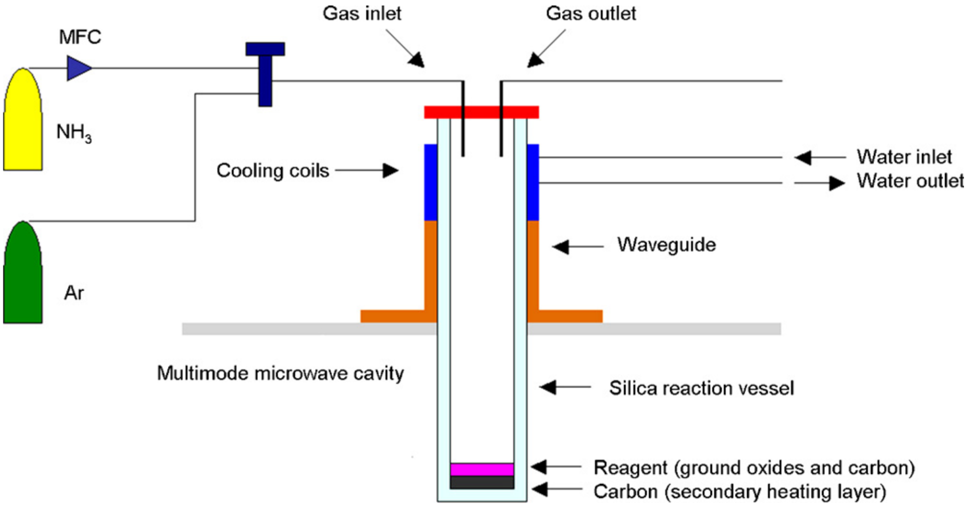

Fig. 1. Schematic of the modified DMO MW-CRAC reactor.

barriers caused by formation of surface layers.[13,14] Heating by microwaves requires that at least one of the reactants couple effectively with the microwave field, i.e. be good susceptors of microwaves at room temperature. The ability of a material to be heated by microwave absorption is proportional to its loss tangent ($\tan\delta$). The loss tangent is a function of two dielectric properties of the material, both of which are temperature and microwave frequency dependant[11] (Eq. (1)).

$$\tan\delta = \frac{\varepsilon''}{\varepsilon'} \quad (1)$$

where ε' is the relative permittivity and ε'' is the dielectric loss of the material.

The total power absorbed per unit volume (P) of a material by the absorption of microwave energy is given by (Eq. (2))[15]:

$$P = 2\pi f \varepsilon_0 \varepsilon_r' \tan\delta |E|^2 \quad (2)$$

where f is the microwave frequency, ε_0 is the permeability of free space, $\varepsilon_r{}'$ is the relative dielectric constant and E is the magnitude of the internal electric field.

Amorphous carbon is particularly effective at coupling with microwaves[10] and hence carbon can act not only as a reactant in the formation of carbides but also as a susceptor and secondary heat source sustaining the high temperatures required for processes such as reduction and carburisation.[16,17] Microwave methods have been demonstrated to be effective in the synthesis of binary nitrides *via* ammonolysis.[10] In this paper, we describe how by using a bespoke microwave reactor system, it is possible to develop the processes of microwave carbothermal reduction–carburisation and microwave ammonolysis to synthesise quaternary transition metal carbonitrides. We report how this technique has been successful in preparing the new bimetallic carbonitrides $V_{1-x}Ti_x(C,N)$ on timescales that are dramatically reduced over the conventional high temperature, energy intensive methods for synthesis of TM carbides and nitrides.

2. Experimental

Compositions of $V_{1-x}Ti_x(C,N)$ $(0 \leq x \leq 0.4)$ were prepared by MW-CRAC methods using a reactor designed taking a modified domestic microwave oven (DMO) as a basis (Fig. 1). The reactor design enables reactions under anaerobic conditions and control over feed gases and flow rates facilitating both solid-state and solid–gas phase reaction chemistry in a microwave field. The gas-tight silica reaction vessel is inserted into a modified DMO (Panasonic NN-T535 operating at 2.45 GHz; maximum power output 1 kW) through a Cu waveguide and cooling coils constructed around the reaction vessel external aperture and outside the DMO cavity itself. The reaction vessel is inserted into a position where the sample is located at a point of high field intensity within the cavity, i.e. a mode. The reactor vessel itself can be removed to allow handling in an inert atmosphere glove box (either N_2 or Ar). The DMO used is capable of scaleable power inputs of 440, 600, 900 or 1000 W as opposed to varying pulse durations at full power.

For the synthesis of the quaternary carbonitrides, stoichiometric amounts of the respective oxide powders V_2O_5 (Sigma–Aldrich 99.6%) and TiO_2 (Sigma–Aldrich 99.95+ %) were ground in a 2:1 weight ratio with amorphous carbon (BDH > 99.5%; i.e. C excess), where the latter is intended to act as reductant, carbon source and MW susceptor. The powdered reagents (typically *ca.* 160 mg) were placed atop an additional, identical quantity of amorphous carbon that acted as a secondary hearing layer. This ensemble was contained in a gas-tight silica reaction tube which was inserted into the modified DMO apparatus and subsequent reactant gas flow was set using a mass flow controller. In all cases, the reactor was flushed with NH_3 (BOC 99.99%) for 10 min prior to heating. A flow of 120 ml min^{-1} of NH_3 was maintained during heating and cooling. The reactor was subsequently flushed with argon (BOC 99.995%) for an additional 5 min before the product was retrieved. The reaction time, applied power and number of cycles required for the synthesis of various compositions are shown in Table 1. Samples were reground after each cycle as required.

Table 1
Reaction conditions for $V_{1-x}Ti_x(C,N)$ samples.

Sample identifier	Composition, *x*	Cycle time (min)	Power (W)	No reaction cycles
1	0	30	900	1
2	0.1	27	900	1
3	0.2	24	1000	3
4	0.3	24	1000	4
5	0.4	24	1000	4

The products were characterised by powder X-ray diffraction (XRD) using a Philips X'pert $\theta - 2\theta$ diffractometer (with PW 1130 generator operating at 40 kV and 40 mA) with Cu (Kα) radiation. A step size of 0.02° 2θ and step time of 4 s was used over a range of $20° \leq 2\theta \leq 100°$. Scanning electron microscopy (SEM) and energy dispersive X-ray analysis (EDX) was conducted using a JEOL 6400 scanning electron microscope operating at 20 kV with a Noran EDX microanalysis system.

To permit EDX analysis two different methods of sample preparation were used. The first method (i) was to mount the powdered samples onto carbon tabs allowing both SEM and EDX analysis of vanadium and titanium concentrations across the bulk of the samples and from individual particles (area and point scans, respectively). This method however, did not allow accurate evaluation of carbon present in the samples (either in the carbide or from possible excess starting material).

In order to determine the presence and nature of carbon within the samples, a second preparatory method (ii) was devised. Excess carbon was floated off from the products by sonication of *ca*. 50 mg of the mixture in 200 ml deionised water. The suspensions containing the products were then separated from the unreacted carbon using a separating funnel. In order to confirm the floating process was adequate in the removal of unreacted carbon, a control sample of VN (Aldrich 99.6+%) was ground with carbon in a 2:1 weight ratio (carbon:VN). The carbon added was then floated off using the same method. The experimental (**1**–**5**) and control sample suspensions were dried onto a clean aluminium surface ready for SEM and EDX analysis. EDX measurements of the VN control sample confirmed that only trace amounts of carbon were present and hence in all likelihood any carbon detected in the experimental samples originates from carbidic C.

Using method (i), analysis of many thousands of particles simultaneously (over a 4×10^4 μm^2 area) was used to determine the bulk V and Ti stoichiometry of **1**–**5**. Spot analysis (over a 20 μm^2 area) of various individual particles was also taken at progressive stages of the reactions. Comparison of the V *vs.* Ti distribution was used to examine how the product composition and homogeneity varied with reaction cycles and intermediate grindings. Method (ii) was used to establish the presence of nitrogen (qualitatively) and carbon (semi-quantitatively) within individual particles of samples **1**–**5**.

3. Results and discussion

In all reactions, arcing across the sample was seen within 2–5 s of MW application. The samples began to glow brightly within 5–10 s and reached a maximum luminous intensity (yellow/white) within 30 s and thereafter sustained a bright glow throughout the reaction. Products were sintered grey powders (becoming lighter in colour with increasing *x*) with unreacted amorphous carbon still present. The latter was easily physically separated from the products.

A series of sequential reductions to the lower oxides of the constituent metals has been previously observed in the carbothermal reduction of titanium and vanadium oxides.[8,14] These reduction processes are seen to be followed by less well defined stages of either nitridation or carburisation respectively.[10,18,19] The reaction scheme for the carbothermal reduction of the oxides is reported to include intermediate steps such as:

$$2V_2O_5(s) + C(s) \rightarrow 4VO_2(s) + CO_2(g) \quad (3)$$

$$2VO_2(s) + C(s) \rightarrow V_2O_3(s) + CO_2(g) \quad (4)$$

and,

$$4TiO_2(s) + C(s) \rightarrow Ti_4O_7(s) + CO(g) \quad (5)$$

$$3Ti_4O7(s) + C(s) \rightarrow 4Ti_3O_5(s) + CO(g) \quad (6)$$

respectively.

Although we did not analyse the evolution of products of reactions for **1**–**5** at low time steps systematically, we observed from PXD that for reactions performed at reduced power and/or reduced reaction times, mixtures of lower TM oxides of vanadium and titanium dominated the products. For vanadium, V_2O_5 was reduced to VO_2 and V_2O_3 as is observed in the conventional carbothermal process. TiO_2 appears to reduce to a number of TiO_{2-x} (e.g. defect rutile and Magnelli) phases. Hence several intermediate reduction products are formed prior to the carburisation and ammonolysis stages and the formation of the quaternary V–Ti–C–N solid solution phases.

Final products of the $V_{1-x}Ti_x(C,N)$ system were characterised by XRD. Patterns for **1** – **5** are shown in Fig. 2a. The diffraction patterns of **1**–**5** show characteristic peaks of an NaCl-type structure with a shift in the peak positions towards lower 2θ values as *x* increases, commensurate with an increase in the cell parameter, *a*. The Bragg peaks are broadened and become increasingly asymmetric with increasing Ti content (**1**–**5**) as shown for the (1 1 1) reflections in Fig. 2b. These reflections could be fitted using a pseudo Voigt function with an empirical asymmetry correction as implemented in the CMPR suite of programs.[32] Due to the broadness of the peaks, and the relatively low diffraction angle, the contribution of α_1/α_2 splitting to the peak shape was not explicitly addressed. This approach provides a straightforward way of assessing the change in peak shape

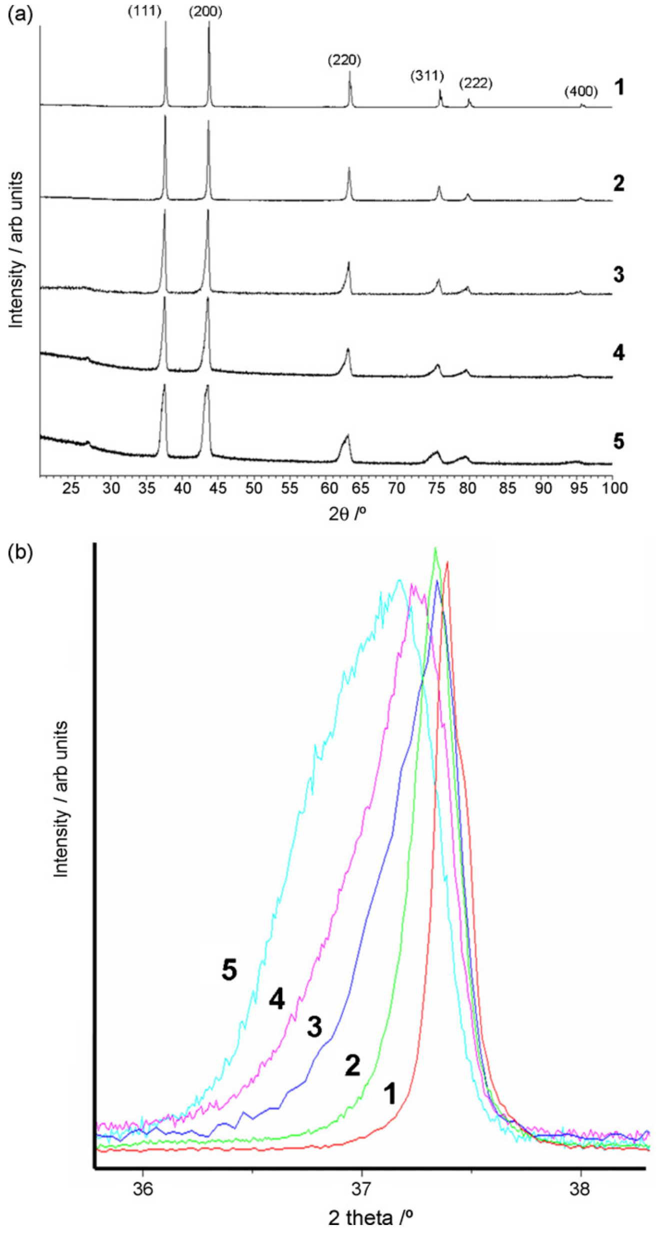

Fig. 2. XRD patterns (a) of products $V_{1-x}Ti_x(C,N)$, **1**–**5** over the entire 2θ range and (b) showing the (1 1 1) reflection for **1**–**5**.

between the five samples. The ability to fit the peaks in this manner suggests that the broadening may arise from microstructural strain or crystallite size effects.

It is, of course, not possible to rule out the presence of two or more phases of very similar lattice parameters arising from small inhomogeneities in composition. This possibility was investigated by following the evolution of peak shape with heating.

A sample of $V_{0.8}Ti_{0.2}(C,N)$ was heated for four discrete heating cycles of 40 min at 600 W. X-ray diffraction patterns were collected after each heating cycle and showed that the peaks became narrower and more symmetric with extended heating until the third cycle when the peak shape was the same as **3** and further heating caused no changes in the diffraction profile. This temporal evolution in peak shape suggests that the sample initially contains two or more rock salt phases with differing compositions. Further heating of the sample provides additional time for mass transport to occur and this leads to narrowing of the Bragg peaks as the sample composition becomes more homogeneous. The absence of further peak narrowing suggests that the thermodynamic product has been obtained and that no significant compositional variation remains in the sample. This inference finds strong support from the spatially resolved composition measurements obtained from the EDX data described below.

Table 2
Refined lattice parameters for $V_{1-x}Ti_x(C,N)$ samples.

Sample	Ti content, x	a (Å)
1	0	4.1625 (3)
2	0.1	4.1689 (3)
3	0.2	4.1768 (9)
4	0.3	4.1863 (4)
5	0.4	4.201 (1)

Reflections were indexed and lattice parameters refined by least squares methods[20] using the software package DICVOL.[21] The refined cell parameters are shown in Table 2. The lattice parameter increases progressively with x commensurate with replacement of vanadium by larger titanium atoms within the mixed metal carbonitride solid solution. This trend is consistent with the cell volumes (a parameters) of both the respective binary nitrides and carbides, assuming stoichiometric compositions, *viz*. VN ($a = 4.137(1)$ Å) [22] *vs*. TiN ($a = 4.2417(12)$ Å) [23] and VC ($a = 4.172(3)$ Å) [24] *vs*. TiC ($a = 4.328(2)$ Å). [25] As each of the binary compounds (VN, TiN, VC and TiC) is reported as fully mutually soluble,[6,7] it should be possible to interpolate between the lattice parameters of the bimetallic nitrides and carbides ($V_{1-x}Ti_xN(C)$) and the monometallic carbonitrides ($Ti(V)C_{1-y}N_y$) to derive theoretical lattice parameters for members of the pseudo-quaternary solid solution $V_{1-x}Ti_xC_{1-y}N_y$, assuming the behaviour of the systems follow Vegard's law. This is a reasonable assumption since members of the Ti–Nb–C–N solid solution system follow such a relationship[26] and the limited data for TiC–TiN and VC–VN suggest linear variation with mole fraction.[6] More recent studies of Ti(C,N) materials produced by high energy ball milling are in line with these earlier observations.[27]

Fig. 3a demonstrates that the lattice parameters of **1**–**5** follow an approximately linear relationship with Ti content, x and are indeed consistent with Vegard's law. Fig. 3b interposes the lattice parameters of the Ti–V–N–C solid solution within the V–N–C, Ti–N–C, V–Ti–N and V–Ti–C phase space. From this representation (Fig. 3b) it is apparent that the ternary systems V–Ti–N and V–Ti–C also follow approximately linear relationships with metal content, although the slopes are of differing gradient. The differences in slope and deviation from linearity in all these systems might be rationalised in terms not simply of metal stoichiometry, of course, but also of non-metal stoichiometry plus an additional factor of defects (vacancies) on the non-metal sub-lattice. Such a departure from ideal (1:1) stoichiometry is well known in the binary TM carbides and nitrides (MC_{1-y}, MN_{1-y}; typically y can be as large as 0.5 while retain-

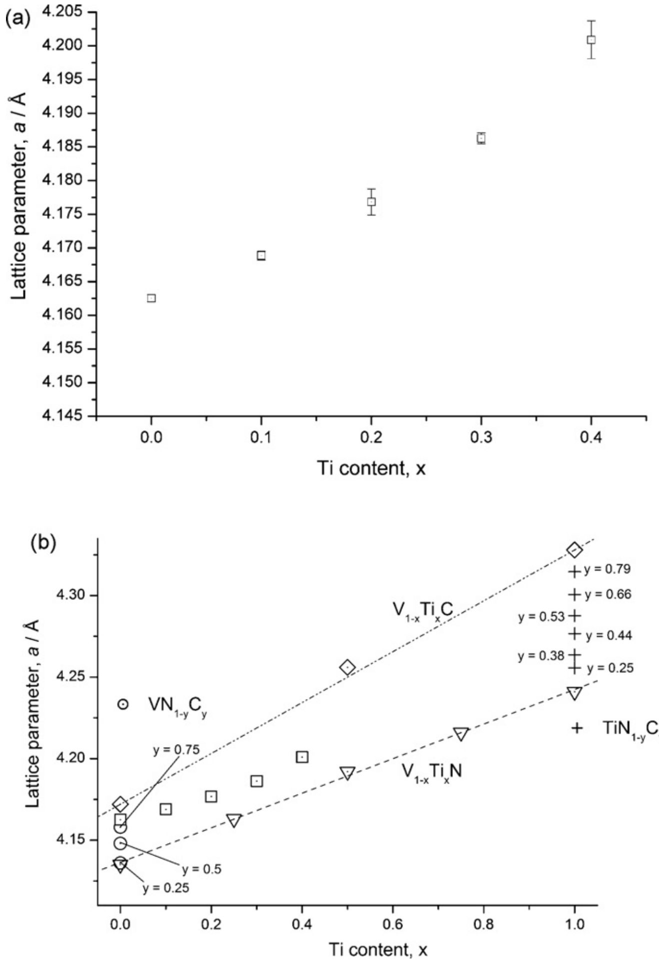

Fig. 3. Lattice parameter *a vs. x* within the V–Ti–N–C phase field showing (a) experimental data for **1**–**5**, $V_{1-x}Ti_x(C,N)$ (squares) and (b) data for **1**–**5** against data for previously reported $V_{1-x}Ti_xN_{1-y}C_y$ compounds: $V_{1-x}Ti_xC$ (diamonds [24,25,29]); $V_{1-x}Ti_xN$ (triangles [28]); $VN_{1-y}C_y$ (circles [28]); $TiN_{1-y}C_y$ (crosses[27]). The approximate linear fits to *a vs. x* for the systems $V_{1-x}Ti_xC$ and $V_xTi_{1-x}N$, respectively are indicated.

Table 3
EDX area scan measurements.

Sample	Ti content, *x*	Nominal V:Ti ratio	V:Ti (+/−%) ratio by EDX
1	0.0	100:0	100:0 (−)
2	0.1	90:10	91:9 (1)
3	0.2	80:20	80:20 (1)
4	0.3	70:30	70:30 (2)
5	0.4	60:40	61:39 (2)

ing the rock salt structure), but has not been explored in any detail for multimetallic compounds or for TM carbonitrides. Existing studies of the binary systems alone can be somewhat inconsistent. For example, in the TiC_{1-y} series, the maximum lattice parameter has been reported to occur for $TiC_{0.85}$ (which itself is only marginally greater than *a* for TiC).[7] By contrast, for TiN_{1-y}, rock salt nitrides are reported to form for $y \leq 0.5$ with *a* reaching a maximum at $y = 0$.[7] Notably, the VC_{1-y} system is reported to reach a maximum carbon content at $y = 0.9$.[31] Nevertheless, the decrease in lattice parameter with increasing nominal anion vacancy concentration is one generally reproduced throughout interstitial rock salt TM carbides and nitrides.[7,30]

Unfortunately, combustion (CHN; Carbon, Hydrogen, Nitrogen) analysis of **1**–**5** proved inconclusive in quantitatively determining the carbon and nitrogen composition (although the presence of both elements was substantiated). The data for both the bimetallic carbide and the nitride systems in Fig. 3b show a linear relationship between lattice parameter and metal content. However, the substitution of Ti for V leads to a more rapid increase in the lattice parameter for the carbides than in the nitride series. All compounds adopt the rock salt structure and so the metal–anion distances are constrained $^a/_2$ by the high site symmetry of the metal and anion positions. The fact that the rate of change of *a vs. x* for the V–Ti–N–C system (**1**–**5**) is different from either the V–Ti–C or V–Ti–N compounds suggests that the degree of carburisation *vs.* nitrogenation and/or vacancy inclusion is not a constant for the given reaction conditions (cycle numbers and irradiation times). The carbon *vs.* nitrogen concentrations cannot be deduced/interpolated from the XRD data, as possible anion vacancy effects on the lattice parameter cannot be de-convoluted. In fact, more generally, a systematic study of TM pseudo-ternary and quaternary carbides, nitrides and carbonitrides correlating composition (stoichiometry), structure and both functional and structural properties is a requirement of some urgency if links between properties and bonding (electronic structure) are to be understood and manipulated. Elemental analysis and XRD alone are not sufficient to address these complex relationships, whereas powder neutron diffraction is an effective probe of light non-metals and vacancies. The approach is one we are to pursue for the Vi–Ti–C–N system and other complex carbide–nitride families.

SEM images show agglomerated plate like structures for **1**–**5**, with individual platelets and irregular crystallites ranging in size from *ca.* 250 nm to 5 μm. Aggregated particles usually measured 5-30 μm in width. No significant change in size or morphology of the structures was apparent for each of **3**–**5** from one heating cycle to the next. Representative micrographs are shown in Fig. 4.

EDX using preparation method (i) (see Section 2) was used successfully to determine the metal ratios present across the bulk samples and to investigate the compositional distribution of the metals across discrete areas of individual particles with reference to the number of heating cycles used in the synthesis. Analysis across 4×10^4 μm^2 areas confirmed the intended ratios of V and Ti for **1**–**5** (Table 3).

Comparison was also made of the ratios of vanadium and titanium present within selected 20 μm^2 areas – typically covering up to 10 individual particles – to determine the degree of homogeneity in the metal distribution (as assessed by the mean and standard deviation of Ti content, *x* across 7–10 particles) with heating cycle number. These measurements show that the variability in titanium content between different particles in a sample is largely independent of *x*. This provides strong evidence that inhomogeneous variation in metal content is not responsible for the peak broadening observed in the X-ray diffraction profiles for larger values of *x*. One alternative to crystallinity and size/strain effects as the origin of the peak shape is stoichiometric variation

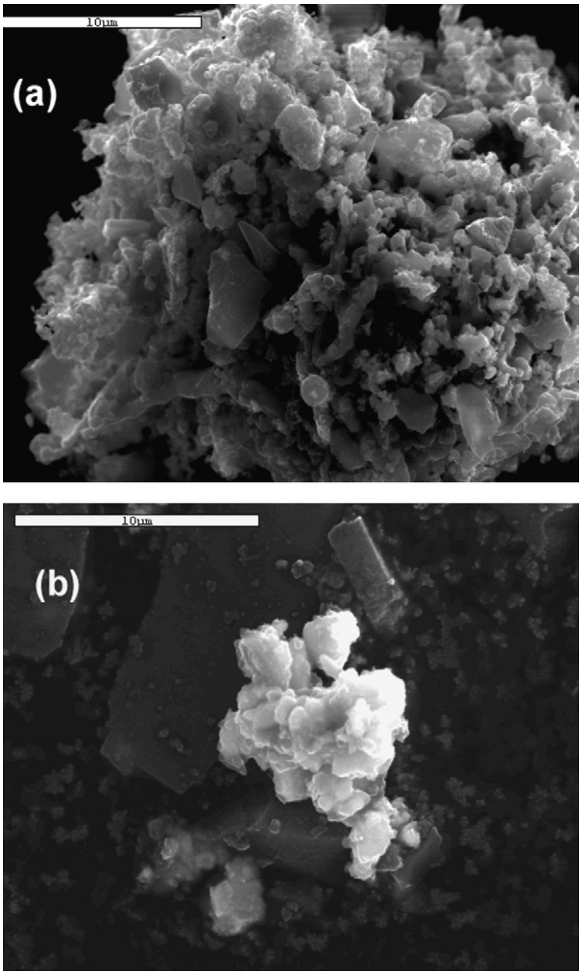

Fig. 4. SEM micrographs of typical morphology seen for $V_{1-x}Ti_x(C,N)$ samples. Shown are images of (a) **3** and (b) **5**.

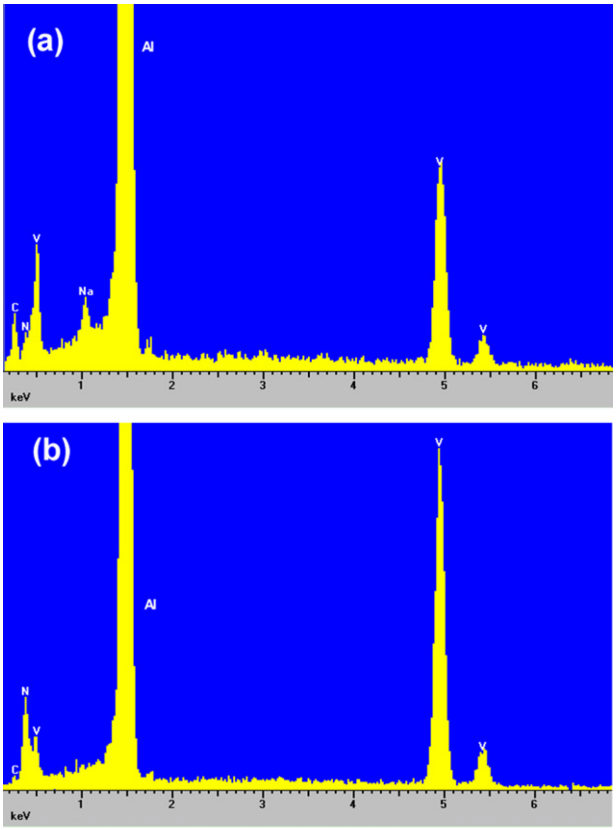

Fig. 5. EDX spectra of (a) **1** post carbon-floating process and (b) a VN + carbon reference sample post carbon-floating process.

in the non-metal content. This is not unreasonable given that the nitrogen content is governed by a solid–gas reaction; there could thus be a concentration gradient from the top to the bottom of the sample under non-equilibrium conditions and an increase in nitrogen stoichiometry with an increased number of heating cycles.

Precise measurement of carbon composition is not possible *via* a conventional EDX experiment where an SEM sample is mounted on a carbon surface. Further, the titanium L-edge overlaps regions of the spectrum where nitrogen K-edge peaks would be observed, rendering the quantitative determination of the nitrogen content difficult. Qualitative analysis of the carbon and nitrogen content present within **1**–**5**, however, is possible by EDX using method (ii) as described in Section 2. Representative EDX spectra are shown in Fig. 5 of both **1**, V(C,N), with unreacted carbon floated off, and a reference sample of (VN + carbon) with carbon then removed using the same method. A characteristic peak of the Al support can be seen in both spectra at 1.45 keV. EDX data indicate that all samples are free of oxygen contamination.

Vanadium, carbon and nitrogen are all found when examining discrete particles of the V(C,N) product after the excess carbon has been removed by flotation (Fig. 5a). (A sodium impurity; almost certainly from handling can also be seen here). By contrast, although vanadium and nitrogen are clearly observed, negligible levels of carbon are detected in the VN reference sample after flotation (Fig. 5b). Hence the EDX data support the conclusion that carbon in **1**–**5** is intrinsic to the main phase and that **1**–**5** are quaternary carbonitrides.

Previous work describing the use of modified DMO apparatus for the synthesis of binary nitrides reported carbothermal nitrogenation occurred with no evidence of carburisation.[10] It has been reported that during the carbothermal nitridation of vanadium (*via* inductive heating), the formation of the carbide occurs only when the initial carbon content exceeds a molar ratio of 1:5 V_2O_5:C and increases proportionally with increasing carbon thereafter.[18] Comparable initial oxide:carbon molar ratios were employed during our experiments with the additional presence of the separate carbon layer (Fig. 1) which was not intimately mixed with the oxide precursors. Our experimental evidence indicates that sufficient carbon is present to drive the formation of the carbonitrides rather than the nitrides. It does appear, however, that longer reaction times (increased heating cycles) lead to further nitriding and that a reaction sequence of reduction–carburisation–nitridation probably exists with the current configuration of our experiments. This is a premise we aim to test in future *in situ* experiments.

We are currently pursuing ways to optimise these reactions and to measure and control the levels of carbon and nitrogen inclusion both within this system and within a wider variety of other mixed transition metal carbonitrides. By exerting these greater levels of non-metal control, it should be possible to tune both electronic and structural (mechanical) properties. This is an exciting prospect and one we are considering in our current research.

4. Conclusion

Bimetallic carbonitrides, $V_{1-x}Ti_x(C,N)$, have been synthesised as a solid solution over a compositional range of $0 \leq x \leq 0.4$. The materials have been rapidly synthesised *via* a carbothermal reduction–ammonolysis/carburisation (MW-CRAC) method under direct microwave heating and controlled atmospheres using a modified DMO reactor. Total reaction times are an order of magnitude quicker than using conventional methods used for synthesis of the constituent monometallic carbides and nitrides.[33]

XRD and EDX data support the conclusion that mixed metal carbonitrides are being formed. Increasing numbers of heating cycles are required to achieve a homogeneous metal distribution in compositions of increasing titanium concentration (x). We speculate that variation in the homogeneity of the anion stoichiometry may be one cause of XRD peak asymmetry and that C:N ratios may be determined by reaction duration (number of heating cycles).

Acknowledgements

DHG and IH thank the University of Nottingham for a studentship for CPW. EJC thanks the Royal Society for a University Research Fellowship.

References

1. Wiener, G. W. and Berger, J. A., Structure and magnetic properties of some transition metal nitrides. *J. Met.*, 1955, **7**, 360–368.
2. Oyama, S. T., *The Chemistry of Transition Metal Carbides and Nitrides*. Chapman and Hall, London, 1996.
3. Kou, X. C., Qiang, W. J. and Kronmüller, H., Coercivity of Sm-Fe-N ferromagnets produced by the mechanical alloying technique. *J. Appl. Phys.*, 1993, **7**, 6791–6797.
4. Qui, C. H., Hoggart, C., Melton, W., Leksono, M. W. and Pankove, J. I., Study of defect states in GaN films by photoconductivity measurement. *Appl. Phys. Lett.*, 1995, **66**, 2712–2714.
5. Ramanathan, S. and Oyama, S. T., New catalysts for hydroprocessing: transition metal carbides and nitrides. *J. Phys. Chem.*, 1995, **49**, 16365–16372.
6. Duwez, P. and Odell, F., Phase relationships in the binary systems of nitrides and carbides of zirconium, columbium, titanium, and vanadium. *J. Electrochem. Soc.*, 1950, **97**, 299–304.
7. Pierson, H., *Handbook of Refractory Carbides and Nitrides*. Noyes Publications, Westwood, 1996.
8. Xiang, D. P., Lui, Y., Zhao, Z. W., Cao, H., Gao, S. J. and Tu, M. J., Reaction sequences and influence factors during preparation of Ti(C,N) powders. *J. Alloy. Compd.*, 2007, **429**, 264–269.
9. Clark, D. E. and Foltz, D. C., *Microwave Processing of Materials*. National Academies Press, Washington, 1994.
10. Vaidhyanathan, B. and Rao, K. J., Synthesis of Ti, Ga, and V nitrides: microwave-assisted carbothermal reduction and nitridation. *Chem. Mater.*, 1997, **9**, 1196–1200.
11. Gabriel, C., Gabriel, S., Grant, E. H., Halstead, B. S. J. and Mingos, D. M. P., Dielectric parameters relevant to microwave dielectric heating. *Chem. Soc. Rev.*, 1998, **27**, 213.
12. Meek, T. T., Holcombe, C. E. and Dykes, N., Microwave sintering of some oxide materials using sintering aids. *J. Mater. Sci. Lett.*, 1987, **6**, 1060–1062.
13. Wei, P., Quing, Y. and Juan, C., Mechanism of carbothermal synthesis of aluminium nitride. *Thermochem. Acta*, 1999, **325**, 89–93.
14. Houmes, J. D. and ur Loye, H.-C, Microwave synthesis of ternary nitride materials. *J. Solid State Chem.*, 1997, **130**, 266–271.
15. Clark, D. E., Folz, D. C. and West, J. K., Processing materials with microwave energy. *Mater. Sci. Eng. A*, 2000, **287**, 153–158.
16. Hassine, N. A., Binner, J. G. P. and Cross, T. J., Synthesis of refractory metal carbide powders via microwave carbothermal reduction. *Int. J. Ref. Met. Hard Mater.*, 1995, **13**, 353–358.
17. Vallance, S. R., Kingman, S. and Gregory, D. H., Ultra-rapid materials processing: synthesis of tungsten carbide, WC, in sub-minute timescales. *Adv. Mater.*, 2007, **19**, 138–142;
    Vallance, S. R., Kingman, S. and Gregory, D. H., Ultra-rapid processing of refractory carbides; 20 s Synthesis of molybdenum carbide, Mo_2C. *Chem. Commun.*, 2007, 742–744.
18. Tripathy, P. K., Sehra, J. C. and Kulkarni, A. V., On the carbonitrothermic reduction of vanadium pentoxide. *J. Mater. Chem.*, 2001, **11**, 691–695.
19. Woo, Y.-C., Kang, H.-J. and Kim., J. D., Formation of TiC particle during carbothermal reduction of TiO_2. *J. Eur. Ceram. Soc.*, 2007, **27**, 719–722.
20. Hoff, W. D., Stratton, R. P. and Kitchingman, W. J., Computer determination of accurate lattice parameters from powder diffraction data. *J. Sci. Instrum.*, 1964, **41**, 695–696.
21. Boultif, A. and Louer, D., Powder pattern indexing with the dichotomy method. *J. Appl. Cryst.*, 2004, **37**, 724–731.
22. Gajbhiye, N. S. and Ningthoujam, R. S., Low temperature synthesis, crystal structure and thermal stability studies of nanocrystalline VN particles. *Mater. Res. Bull.*, 2006, **41**, 1612–1621.
23. Wong-Ng, W., McMurdie, H., Paretzkin, B., Hubbard, C. and Dragoo, A., Standard X-ray diffraction powder patterns of sixteen ceramic phases. *Powder Diffract. J.*, 1987, **2**, 191–203.
24. Pflueger, J., Fink, H. J., Weber, W., Bohnen, K. P. and Crecelius, G., Dielectric properties of TiC_x, TiN_x, VC_x, and VN_x from 1.5 to 40 eV determined by electron-energy-loss spectroscopy. *Phys. Rev. B*, 1984, **30**, 1155–1163.
25. Christensen, A. N., The temperature factor parameters of some transition metal carbides and nitrides by single crystal X-ray and neutron diffraction. *Acta. Chem. Scand. A*, 1978, **32**, 89–90.
26. Córdoba, J. M., Sayagués, M. J., Alcalá, M. D. and Gotor, F. J., Monophasic $Ti_yNb_{1-y}C_xN_{1-x}$ nanopowders obtained at room temperature by MSR. *J. Mater. Chem.*, 2007, **17**, 650–653.
27. Córdoba, J. M., Sayagués, M. J., Alcalá, M. D. and Gotor, F. J., Synthesis of titanium carbonitride phases by reactive milling of the elemental mixed powders. *J. Am. Ceram. Soc.*, 2005, **88**, 1760–1764.
28. Kieffer, R., Nowotny, H., Mayer, P. E. and Dufek, G., New investigations concerning miscibility of transition-metal nitrides and carbides. *Metallurgy*, 1972, **26**, 701.
29. Goretzki, G., Neutron diffraction studies on titanium-carbon and zirconium-carbon alloys. *Phys. Status Solidi*, 1967, **20**, 141.
30. Toth, L. E., *Transition Metal Carbides and Nitrides*. Academic Press, New York, 1971.
31. Storms, E. K. and McNeal, R. J., The vanadium-vanadium carbide system. *J. Phys. Chem.*, 1962, **66**, 1401–1408.
32. Toby, B. H., CMPR—a powder diffraction toolkit. *J. Appl. Crystallogr.*, 2005, **38**, 1040–1041.
33. Choi, J. G., Ha, J. and Hong, J., Synthesis and catalytic properties of vanadium interstitial compounds. *Appl. Catal. A*, 1998, **168**, 47–56.